Non-thermal CMSSM with a 125 GeV Higgs

Luis Aparicio,[a] **Michele Cicoli,**[a,b,c] **Bhaskar Dutta,**[d] **Sven Krippendorf,**[e]
Anshuman Maharana,[f] **Francesco Muia**[b,c] **and Fernando Quevedo**[a,g]

[a]*ICTP,*
 Strada Costiera 11, Trieste 34014, Italy
[b]*Dipartimento di Fisica e Astronomia, Università di Bologna,*
 via Irnerio 46, 40126 Bologna, Italy
[c]*INFN, Sezione di Bologna,*
 via Irnerio 46, 40126 Bologna, Italy
[d]*Department of Physics and Astronomy,*
 Mitchell Institute for Fundamental Physics and Astronomy, TAMU,
 College Station, TX 77843-4242, U.S.A.
[e]*Rudolf Peierls Centre for Theoretical Physics, University of Oxford,*
 1 Keble Road, Oxford, OX1 3NP, U.K.
[f]*Harish Chandra Research Institute,*
 Chhatnag Road, Jhunsi, Allahabad, UP 211019, India
[g]*DAMTP, Centre for Mathematical Sciences,*
 Wilberforce Road, Cambridge, CB3 0WA, U.K.

 E-mail: laparici@ictp.it, dutta@physics.tamu.edu, mcicoli@ictp.it,
 sven.krippendorf@physics.ox.ac.uk, anshumanmaharana@hri.res,
 muia@bo.infn.it, f.quevedo@damtp.cam.ac.uk

Abstract: We study the phenomenology of the CMSSM/mSUGRA with non-thermal neutralino dark matter. Besides the standard parameters of the CMSSM we include the reheating temperature as an extra parameter. Imposing radiative electroweak symmetry breaking with a Higgs mass around 125 GeV and no dark matter overproduction, we contrast the scenario with different experimental bounds from colliders (LEP, LHC), cosmic microwave background (Planck), direct (LUX, XENON100, CDMS, IceCube) and indirect (Fermi) dark matter searches. The allowed parameter space is characterised by a Higgsino-like LSP with a mass around 300 GeV. The observed dark matter abundance can be saturated for reheating temperatures around 2 GeV while larger temperatures require extra non-neutralino dark matter candidates and extend the allowed parameter space. Sfermion and gluino masses are in the few TeV region. These scenarios can be achieved in string models of sequestered supersymmetry breaking which avoid cosmological moduli problems and are compatible with gauge coupling unification. Astrophysics and particle physics experiments will fully investigate this non-thermal scenario in the near future.

Keywords: Supersymmetry Phenomenology

ArXiv ePrint: 1502.05672

Contents

1 Motivation for non-thermal dark matter

One of the main particle physics candidates for dark matter (DM) is a stable neutralino χ which emerges as the lightest supersymmetric particle (LSP) in several scenarios beyond the Standard Model (SM). The DM relic abundance is generically *assumed* to be produced thermally by the following process: the LSP is in a thermal bath in the early universe, subsequently drops out of thermal equilibrium and freezes-out at temperatures of order $T_f \simeq m_\chi/20$ when DM annihilation becomes inefficient.

However, we have no direct observational evidence of the history of the universe before Big Bang Nucleosynthesis (BBN) for temperatures above $T_{\mathrm{BBN}} \simeq 3\,\mathrm{MeV}$. There is therefore no reason to assume a very simple cosmological history characterised by just a single period of radiation dominance from the end of inflation until BBN. In fact, the presence of a period of matter domination between the end of inflation and BBN could completely change the final prediction for the DM relic density if the reheating temperature at the end of this period of matter dominance is below T_f [1–6].

This non-thermal picture emerges generically in UV theories like string theory due to the ubiquitous presence of gravitationally coupled scalars [7–13]. During inflation these fields, called moduli, get a displacement from their minimum that is in general of order M_P [14]. After the end of inflation, when the Hubble constant reaches their mass, $H \sim m_{\mathrm{mod}}$, they start oscillating around their minimum and store energy. Redshifting as matter, they quickly dominate the energy density of the universe which gets reheated when the

moduli decay. Being only gravitationally coupled, the moduli tend to decay very late when $H \sim \Gamma \sim m_{\mathrm{mod}}^3/M_P^2$. The corresponding reheating temperature

$$T_R \sim \sqrt{\Gamma M_P} \sim m_{\mathrm{mod}} \sqrt{\frac{m_{\mathrm{mod}}}{M_P}}\,, \tag{1.1}$$

has to be larger than T_{BBN} in order to preserve the successful BBN predictions.[1] This requirement sets a lower bound on the moduli masses of order $m_{\mathrm{mod}} \gtrsim 30\,\mathrm{TeV}$ [7–9].

Generically in string compactifications supersymmetry (SUSY) breaking effects develop a mass for the moduli and generate by gravity or anomaly mediation soft terms of order M_{soft}. Due to their common origin, the mass of the lightest modulus m_{mod} is therefore related to the scale of the soft terms as $M_{\mathrm{soft}} = \kappa m_{\mathrm{mod}}$. Given the cosmological constraint $m_{\mathrm{mod}} \gtrsim 30\,\mathrm{TeV}$, only models with $\kappa \ll 1$ can allow for low-energy SUSY to solve the hierarchy problem. Values of $\kappa \sim \mathcal{O}(10^{-2})$ can come from loop suppression factors [17–20] while much smaller values $\kappa \sim \mathcal{O}(10^{-3} - 10^{-4})$ can arise due to sequestering effects [21, 22]. For $M_{\mathrm{soft}} \sim \mathcal{O}(1)\,\mathrm{TeV}$, the corresponding reheating temperature becomes

$$T_R \sim \frac{M_{\mathrm{soft}}}{\kappa^{3/2}} \sqrt{\frac{M_{\mathrm{soft}}}{M_P}} \sim \kappa^{-3/2}\,\mathcal{O}(10^{-2})\,\mathrm{MeV}\,, \tag{1.2}$$

which for $10^{-2} \lesssim \kappa \lesssim 10^{-4}$ is between $\mathcal{O}(10)\,\mathrm{MeV}$ and $\mathcal{O}(10)\,\mathrm{GeV}$. This is below the freeze-out temperature for LSP masses between $\mathcal{O}(100)\,\mathrm{GeV}$ and $\mathcal{O}(1)\,\mathrm{TeV}$ which is $T_f \sim \mathcal{O}(10 - 100)\,\mathrm{GeV}$. Therefore any DM relic density previously produced via the standard thermal mechanism gets erased by the late-time decay of the lightest modulus. In this new scenario, the LSP gets produced non-thermally from the modulus decay.

From a bottom-up perspective, non-thermal cosmological histories can also enlarge the available parameter space of different DM models consistent with direct and indirect detection experiments, due to the presence of the additional parameter T_R. This is appealing as it is very hard to reproduce a correct thermal relic density in the CMSSM/mSUGRA (see for instance [23]) since a Bino-like LSP tends to overproduce DM (apart from some fine-tuned cases like stau co-annihilation and A-funnel or in the case of precision gauge coupling unification [24]) while for a Higgsino- or Wino-like LSP the relic density is in general underabundant (except for cases like well tempered Bino/Higgsino or Bino/Wino DM [25]).

The purpose of this paper is to study non-thermal DM in the CMSSM/mSUGRA where the free parameters are: the standard parameters of the CMSSM/mSUGRA [26–29], i.e. the universal scalar mass m, universal gaugino mass M and trilinear coupling A defined at the GUT scale, $\tan\beta$ and the sign of μ, with in addition the reheating temperature T_R from the decay of the lightest modulus. We shall follow the RG running of these parameters from the GUT to the electroweak (EW) scale and require a Higgs mass $m_h \simeq 125\,\mathrm{GeV}$, a correct radiative EW symmetry breaking (REWSB) and no DM non-thermal overproduction. We shall then focus on the points satisfying all these requirements and we will impose on them several phenomenological constraints coming from LEP [30–33], LHC [34–39], Planck [40], Fermi (pass 8 limit) [41], XENON100 [42], CDMS [43],

---

[1]T_R has also to be lower than the temperature above which the internal space decompactifies [15, 16].

IceCube [44] and LUX [45]. Moreover we shall focus only on cases where the LSP has a non-negligible Higgsino component since Bino-like DM requires a very low reheating temperature which is strongly disfavoured by dark radiation bounds in the context of many string models [46]. Interestingly we shall find that the constraints from Fermi and LUX are very severe and do not rule out the entire non-thermal CMSSM parameter space only for reheating temperatures $T_R \gtrsim \mathcal{O}(1)\,\text{GeV}$. The best case scenario is realised for $T_R = 2\,\text{GeV}$ where a Higgsino-like LSP with a mass around $300\,\text{GeV}$ can saturate the observed DM relic abundance. For larger reheating temperatures the LSP Bino component has to increase, resulting in strong direct detection bounds which allow only for cases with DM underproduction. Values of T_R above $1\,\text{GeV}$ require values of $\kappa \sim \mathcal{O}(10^{-3} - 10^{-4})$ which can be realised only in models where the CMSSM is sequestered from the sources of SUSY breaking [21, 22]. In these models the contribution to gaugino masses from anomaly mediation turns out to be negligibly small and hence is distinct from other scenarios [17–20] where contributions from anomaly mediation are significant and where a Wino LSP can be realised. Apart from DM, these models are very promising since they can be embedded in globally consistent Calabi-Yau compactifications [47–49], allow for TeV-scale SUSY and successful inflationary models [50–52], do not feature any cosmological moduli problem,[2] are compatible with gauge coupling unification and do not suffer from any moduli-induced gravitino problem [54, 55]. Non-standard thermal history using CMSSM was considered in ref. [56] where the entropy due to the decay of the inflaton reduces the thermal relic abundance. In this work, however, we consider that the dark matter particles from the moduli decay constitute the dark matter abundance and the thermal dark matter abundance contribution to the net dark matter content is negligible since T_r is not required to be very close to T_f.

In section 2 we discuss CMSSM soft terms, in section 3 we analyse the non-thermal CMSSM, in section 4 we discuss our results and conclusions are given in section 5.

2 CMSSM soft terms

In a UV completion of the MSSM like string theory, SUSY is spontaneously broken by some dynamical mechanism which generates particular relations between the soft terms via gravity, anomaly or gauge mediation. In the case when the soft terms are universal at the GUT scale, they are given by the scalar mass m, the gaugino mass M, the trilinear coupling A and the bilinear Higgs mixing B. We can generically parameterise these soft terms and the μ parameter at the GUT scale as:

$$m = a\,|M|\,, \quad A = b\,M\,, \quad B = c\,M\,, \quad \mu = d\,M\,, \tag{2.1}$$

where, in a stringy embedding, the coefficients a, b, c and d are functions of the underlying parameters while the gaugino mass M sets the overall scale of the soft terms in terms of the gravitino mass $m_{3/2}$. In order to perform a phenomenological analysis of this scenario

---

[2]Ref. [53] provides a significant bound on moduli masses and the number of e-foldings during inflation which can be a challenge for many models.

one has to follow the renormalisation group (RG) evolution of these soft terms from the GUT to the EW scale and impose the following constraints: a correct REWSB, a Higgs mass of order $m_h \simeq 125\,\text{GeV}$, no DM overproduction and no contradiction with flavour observables and with any experimental result in either particle physics or cosmology.

A viable REWSB can be obtained if at the EW scale the following two relations are satisfied:

$$\mu^2 = \frac{m_{H_d}^2 - m_{H_u}^2 \tan^2 \beta}{\tan^2 \beta - 1} - \frac{m_Z^2}{2}, \tag{2.2}$$

where:

$$\sin(2\beta) = \frac{2|B\mu|}{m_{H_d}^2 + m_{H_u}^2 + 2\mu^2}. \tag{2.3}$$

Given that the requirement of a correct REWSB fixes only the magnitude of μ leaving its sign as free, the parameters (2.1) are typically traded for the standard CMSSM/mSUGRA parameters:

$$m = a\,|M|, \quad A = b\,M, \quad \tan \beta \equiv \frac{\langle H_u^0 \rangle}{\langle H_d^0 \rangle}, \quad \text{sign}(\mu), \tag{2.4}$$

where one runs m, M and A (or a, b and M in our case) from the GUT to the EW scale with a particular choice of $\tan \beta$ and $\text{sign}(\mu)$. Eqs. (2.2) and (2.3) then give the value of B and μ at the EW scale. This is the way in which typical spectrum generators operate.[3] The boundary values of B and μ at the GUT scale which give a correct REWSB can be obtained by running back B and μ from the EW to the GUT scale. In this way we obtain the values of the coefficients c and d. In a viable UV model, these values of c and d have to be compatible with the values allowed by the stringy dynamics responsible for SUSY breaking and the generation of soft terms. The eqs. (2.2), (2.3) are tree level relations. We use loop corrections to these relations in our calculations.

3 Non-thermal CMSSM

As motivated in section 1, we shall consider scenarios where the LSP is produced non-thermally like in the case of string compactifications where the reheating temperature T_R from the decay of the lightest modulus is generically below the thermal freeze-out temperature [10–13]. This reheating temperature represents an additional parameter which has to be supplemented to the standard free parameters of the CMSSM (a, b, M, $\tan \beta$ and the sign of μ). We call this new scenario the 'non-thermal CMSSM' which is characterised by the following free parameters: T_R, a, b, the gaugino mass M, $\tan \beta$ and the sign of μ.

3.1 Non-thermal dark matter relic density

The abundance of DM particles χ produced non-thermally by the decay of the lightest modulus is given by [3–6]:

$$\left(\frac{n_\chi}{s}\right)^{\text{NT}} = \min\left[\left(\frac{n_\chi}{s}\right)_{\text{obs}} \frac{\langle \sigma_{\text{ann}} v \rangle_f^{\text{Th}}}{\langle \sigma_{\text{ann}} v \rangle_f} \sqrt{\frac{g_*(T_f)}{g_*(T_R)}} \left(\frac{T_f}{T_R}\right), Y_{\text{mod}}\, \text{Br}_\chi\right], \tag{3.1}$$

---

[3]Here we use `SPheno` v3.3.3 [85, 86].

where g_* is the number of relativistic degrees of freedom, $\langle \sigma_{\mathrm{ann}} v \rangle_f^{\mathrm{Th}} \simeq 2 \times 10^{-26} \mathrm{cm}^3 \, \mathrm{s}^{-1}$ is the annihilation rate at the time of freeze-out needed in the thermal case to reproduce the observed DM abundance:

$$\left(\frac{n_\chi}{s} \right)_{\mathrm{obs}} = \left(\Omega_\chi h^2 \right)_{\mathrm{obs}} \left(\frac{\rho_{\mathrm{crit}}}{m_\chi s h^2} \right) \simeq 0.12 \left(\frac{\rho_{\mathrm{crit}}}{m_\chi s h^2} \right), \tag{3.2}$$

whereas the yield of particle abundance from modulus decay is:

$$Y_{\mathrm{mod}} \equiv \frac{3 T_R}{4 m_{\mathrm{mod}}} \sim \sqrt{\frac{m_{\mathrm{mod}}}{M_P}}. \tag{3.3}$$

Br_χ denotes the branching ratio for modulus decays into R-parity odd particles which subsequently decay to DM.

The expression (3.1) leads to two scenarios for non-thermal DM:

1. 'Annihilation scenario': in this case the DM abundance is given by the first term on the right-hand side of eq. (3.1) and the DM particles undergo some annihilation after their initial production by modulus decay. In order to avoid DM overabundance one needs

$$\langle \sigma_{\mathrm{ann}} v \rangle_f \geq \langle \sigma_{\mathrm{ann}} v \rangle_f^{\mathrm{Th}} \sqrt{\frac{g_*(T_f)}{g_*(T_R)}} \left(\frac{T_f}{T_R} \right). \tag{3.4}$$

Given that $T_R < T_f$ and $g_*(T_R) < g_*(T_f)$, this scenario requires $\langle \sigma_{\mathrm{ann}} v \rangle_f > \langle \sigma_{\mathrm{ann}} v \rangle_f^{\mathrm{Th}}$ as in the case of thermal underproduction. This condition is satisfied by a Higgsino- or Wino-like LSP but not by a pure Bino-like LSP which would generically lead to non-thermal overproduction (apart from the aforementioned cases). However, given that we shall focus on models with just gravity mediated SUSY breaking (contributions from anomaly mediation are subleading) and universal gaugino masses at the GUT scale as in [21, 22], the LSP can never be Wino-like due to the RG running of the gauginos. Bino is the lightest gaugino. Moreover a Wino-like LSP has a significantly larger annihilation cross section than a Higgsino-like LSP resulting in a strong conflict with Fermi bounds for sub-TeV Wino-like DM [57]. In this context, the 'Annihilation scenario' requires a Higgsino-like DM. Let us finally point out that the non-thermal DM relic density can be written in terms of the thermal one as:

$$\Omega_\chi^{\mathrm{NT}} h^2 = \sqrt{\frac{g_*(T_f)}{g_*(T_R)}} \left(\frac{T_f}{T_R} \right) \Omega_\chi^{\mathrm{Th}} h^2. \tag{3.5}$$

For $5 \, \mathrm{GeV} < T_f < 80 \, \mathrm{GeV}$ (corresponding to $100 \, \mathrm{GeV} < m_\chi < 1.6 \, \mathrm{TeV}$), the top, the Higgs, the Z and the $\mathrm{W}^\pm$ are not relativistic, giving $g_*(T_f) = 86.25$ and:

$$\Omega_\chi^{\mathrm{NT}} h^2 = 0.142 \sqrt{\frac{10.75}{g_*(T_R)}} \left(\frac{m_\chi}{T_R} \right) \Omega_\chi^{\mathrm{Th}} h^2. \tag{3.6}$$

2. 'Branching scenario': in this case the DM abundance is given by the second term on the right-hand side of eq. (3.1) and the DM particles are produced directly from

the modulus decay since their residual annihilation is inefficient. In this case both large and small cross sections can satisfy the DM content since the annihilation cross section does not have any impact on the DM content. This scenario is very effective to understand the DM and baryon abundance coincidence problem [58–62]. Given that in general we have $\mathrm{Br}_\chi \gtrsim 10^{-3}$,[4] in order not to overproduce DM for LSP masses of order hundreds of GeV, one needs $Y_{\mathrm{mod}} \lesssim 10^{-9}$. This condition requires a very low reheating temperature:

$$T_R \lesssim 10^{-9} m_{\mathrm{mod}} = 10^{-9} \kappa^{-1} M_{\mathrm{soft}} \,. \tag{3.7}$$

For $M_{\mathrm{soft}} \sim \mathcal{O}(1)\,\mathrm{TeV}$ and $\kappa \sim \mathcal{O}(10^{-2} - 10^{-4})$ we find $T_R \lesssim \mathcal{O}(10)\,\mathrm{MeV}$. In order to obtain such a low reheating temperature one has in general to consider models where the modulus coupling to visible sector fields is loop suppressed [13]. However in this case it is very challenging to avoid a large modulus branching ratio into hidden sector light fields like stringy axions [63, 64] and so typically dark radiation is overproduced [46]. Therefore the 'Branching scenario' does not seem very promising from the phenomenological point of view.

3.2 Collider and CMB constraints

Due to the considerations mentioned above, if the LSP is Bino-like we generically get DM overproduction also in the non-thermal case. The CMSSM boundary condition requires Bino to be the lightest among the gauginos. We shall therefore look for particular regions in the non-thermal CMSSM parameter space where the LSP has a non-negligible Higgsino component. We have developed a Monte Carlo programme to find the regions of this parameter space where the LSP is Higgsino-like, the Higgs mass is around $125.5\,\mathrm{GeV}$,[5] REWSB takes place correctly and the following phenomenological constraints are satisfied:

- LEP [30–33] and LHC [34–39] constraints on neutralino and chargino direct production: $m_\chi \gtrsim 100\,\mathrm{GeV}$;

- LHC [34–39] bounds on gluino and squark masses: $m_{\tilde{g}} \gtrsim 1300\,\mathrm{GeV}$;

- LHC constraints from flavour physics: $\mathrm{BR}(B_s \to \mu^+\mu^-)$ [65] and the constraint on $\mathrm{BR}(b \to s\gamma)$ [66];

- Planck data on DM relic density [40].

To avoid complications with the applicability of the standard `Spheno` version, we restrict our scan on the following parameter ranges: $\tan\beta = 1\,\mathrm{to}\,55$, $a = 0\,\mathrm{to}\,10$, $b = -5\,\mathrm{to}\,5$, and the universal gaugino mass at the high scale $M = 0.3 - 3\,\mathrm{TeV}$. The results are shown in figures 1)–(3 for positive μ (the LSP relic density has been calculated using `microOMEGAS` v3 [87]).

---

[4]In this case, the dominant decay mode of moduli is gauge Bosons, $\phi \to gg$. However the gauginos appear in three body final state, i.e., $\phi \to g\,\tilde{g}\tilde{g}$ with $\mathrm{Br}_\chi \gtrsim 10^{-3}$ [58–62].

[5]Both ATLAS and CMS give values of the Higgs mass between 125 and 126 GeV. In what follows, we will consider ranges of values in this region, allowing to some extent for the uncertainty in the spectrum generators as well. Allowing for a larger uncertainty in the Higgs mass does not alter the following results qualitatively.
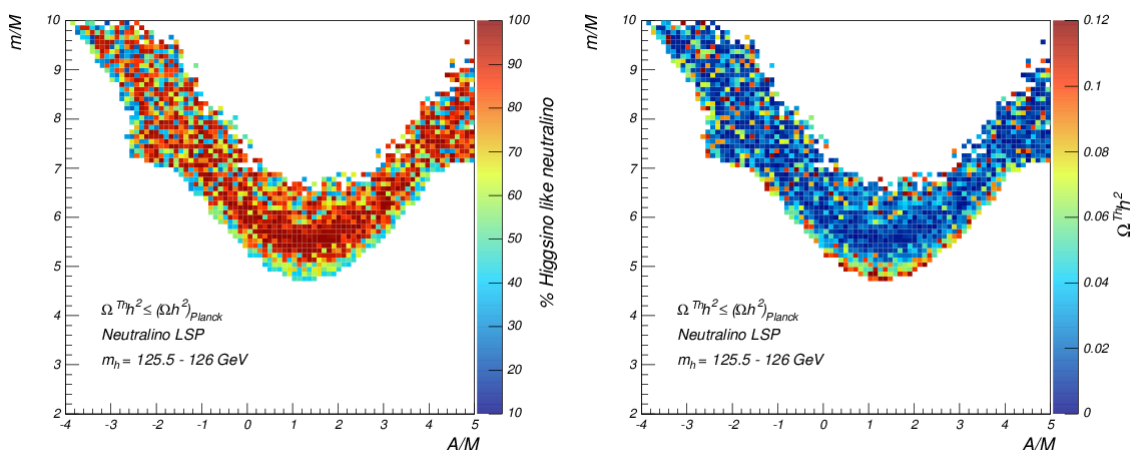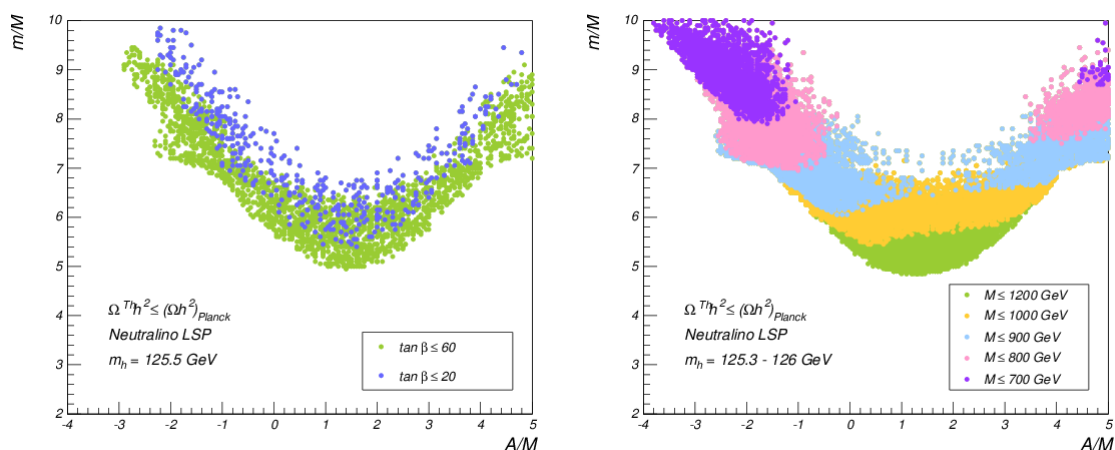
Figure 1. Correlation between $a = m/M$ and $b = A/M$ for different LSP compositions (left) and DM thermal relic densities (right) in the region where the LSP is at least 10% Higgsino.

The plots in figure 1 show the points surviving the above constraints in the A/M-m/M plane (at the GUT scale). The points fit into a V-shaped band illustrating a slight hierarchy between scalar and gaugino masses ($m \gtrsim 5M$) and values of A almost symmetric around $A \simeq M$. The regions shown in the plot are mostly for T_R rather smaller than T_f which keeps mostly the focus point regions in the allowed parameter space. The coannihilation and A-funnel regions can also contribute to the allowed parameter space but they are very fine tuned. The V-shape of our plots is caused by the focus point region which can be obtained by setting $\mu \sim m_Z$ in the EWSB condition with loop corrections. In fact, the dependence of μ^2 on A, M and m arises through $m_{H_u}^2$ which depends on the UV soft terms in the following way: $M^2(f(Q) + g(Q)A/M + h(Q)(A/M)^2 + e(Q)(m/M)^2)$, where f, g, h and e depend on dimensionless gauge and Yukawa couplings (e also includes the tadpole correction from the stop loop) and Q is the SUSY breaking scale [67]. A leading order cancellation in this expression, as needed to achieve a small μ-term in (2.2), gives a V-shaped band in the A/M-m/M plane. We also apply the Higgs mass constraint in this parameter space which depends on the square of $X_t \equiv A_t - \mu \cot\beta$ [68] and X_t^2 preserves the V-shape due to its dependence on $(A/M)^2$.

To illustrate the allowed parameter range and to illustrate different aspects of the surviving points, we show the following plots (for positive sign of μ):

1. In figure 1, the colour codes illustrate the percentage of Higgsino-like neutralino on the left plot and the neutralino contribution to the thermal DM relic density on the right. Note that in most of the points the neutralinos contribute only a small percentage of the total DM relic density and other DM candidates, such as axions, have to be present. The thermal DM relic density is close to the observed Planck value only in a small region corresponding to an LSP that is approximately 50% Bino and 50% Higgsino. However, as we will see in the next section, after imposing indirect detection constraints from Fermi, the only region which survives is the one
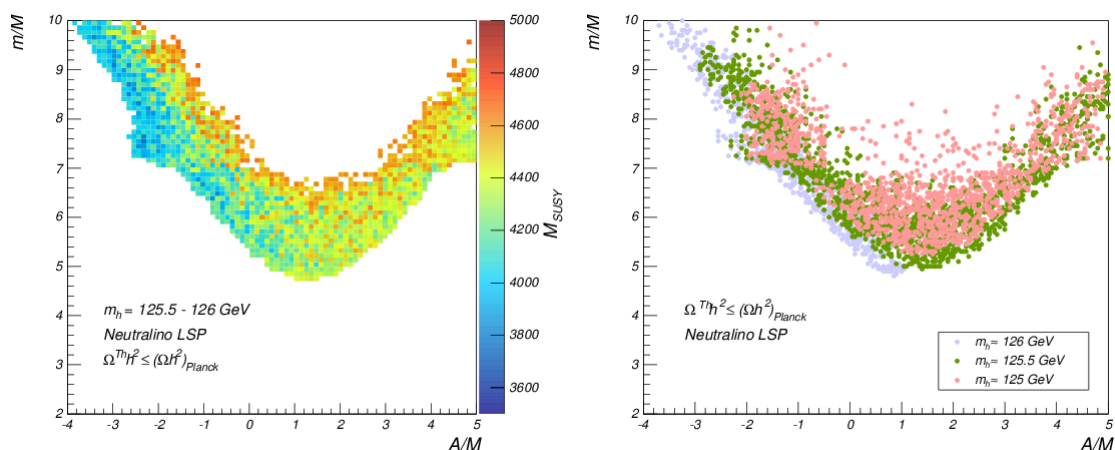
Figure 2. Correlation between $a = m/M$ and $b = A/M$ for different values of $\tan\beta$ (left) and gaugino mass (right) in the region where the LSP is at least 10% Higgsino.

where thermal DM is underabundant (by about 10% of the observed relic density). On the other hand, as we shall see in the next section, non-thermal Higgsino-like DM can lead to larger relic densities which can saturate the Planck value for reheating temperatures around 2 - 3 GeV.

2. The colour codes in figure 2 illustrate the dependence on $\tan\beta$ on the left plot and different values of gaugino masses on the right plot with well-defined domains for different ranges of gaugino masses inside the V-shaped band. Note that $\tan\beta$ tends to have larger values as expected from the fit of m_h and the parameter ranges in this scan. Smaller values of A/M and m/M are preferred for larger gaugino mass due to RG flow of masses to fit the experimental value of m_h.

3. For figure 3 the colours illustrate on the left the different values of the typical scale of SUSY particles M_{SUSY}, defined here as the averaged stop mass $M_{\mathrm{SUSY}}^2 = m_{\tilde{t}_1} m_{\tilde{t}_2}$. Notice that M_{SUSY} is around 4 - 5 TeV. In principle, we could explore values larger than 5 TeV however it would bring us beyond the level of applicability of the spectrum generator `SPheno` we have been using which assume similar values for all soft terms. An analysis for a split-like SUSY case with larger differences between sfermions and gaugino masses would be required in that case but this goes beyond the scope of this article. The colours on the right plot illustrate the dependence on the Higgs mass for which we have taken $m_h = 125, 125.5, 126$ GeV respectively. Note that for $m_h = 126$ GeV there are allowed points only on the left of the V-shaped band because of the above mentioned cut-off on M_{SUSY}. Generally speaking we see that by allowing a larger range for the Higgs mass, we widen the V-shaped region.

Figure 3. Correlation between $a = m/M$ and $b = A/M$ for different values of the averaged stop mass M_{SUSY} (left) and the Higgs mass (right) in the region where the LSP is at least 10% Higgsino.

### 3.3 Direct and indirect detection constraints

In the figures above we have set $\mu > 0$ but their pattern does not change for $\mu < 0$. The next step is to impose the following phenomenological constraints for the separate case of positive and negative μ since the DM direct detection cross section depends on $\text{sign}(\mu)$:

- Fermi bounds on DM indirect detection [41];

- IceCube [44] and XENON100 [42] bounds for spin dependent DM direct detection;

- LUX [45], CDMS [43] bounds on spin independent DM direct detection.

3.3.1 Results for positive μ

If we impose the above constraints, indirect detection bounds turn out to be very severe. Using the new Fermi bounds (pass 8 limit) coming from data collected until 2014 (the pass 7 limit includes only data until 2012), we do not find any allowed point for $T_R \lesssim 2\,\text{GeV}$.

In figure 4 we show the results for different reheating temperatures. The red points show the parameter space where we saturate the DM content measured from Planck [40]. We find more allowed points for $T_R = 10\,\text{GeV}$ compared to $T_R = 2\,\text{GeV}$ since the ratio of T_f/T_R becomes smaller for large T_R, and so a smaller annihilation cross section is needed, resulting in a better chance to satisfy the bounds from Fermi. We only see the large Higgsino dominated regions for smaller T_R since in this case a larger annihilation cross section is needed to saturate the DM content. For larger T_R, an LSP with a smaller Higgsino component becomes allowed (higher Bino component) and this region appears for smaller values of gaugino mass. We finally mention that the Planck constraints on indirect detection through DM annihilation during the recombination epoch are less stringent than those of Fermi for our scenarios.
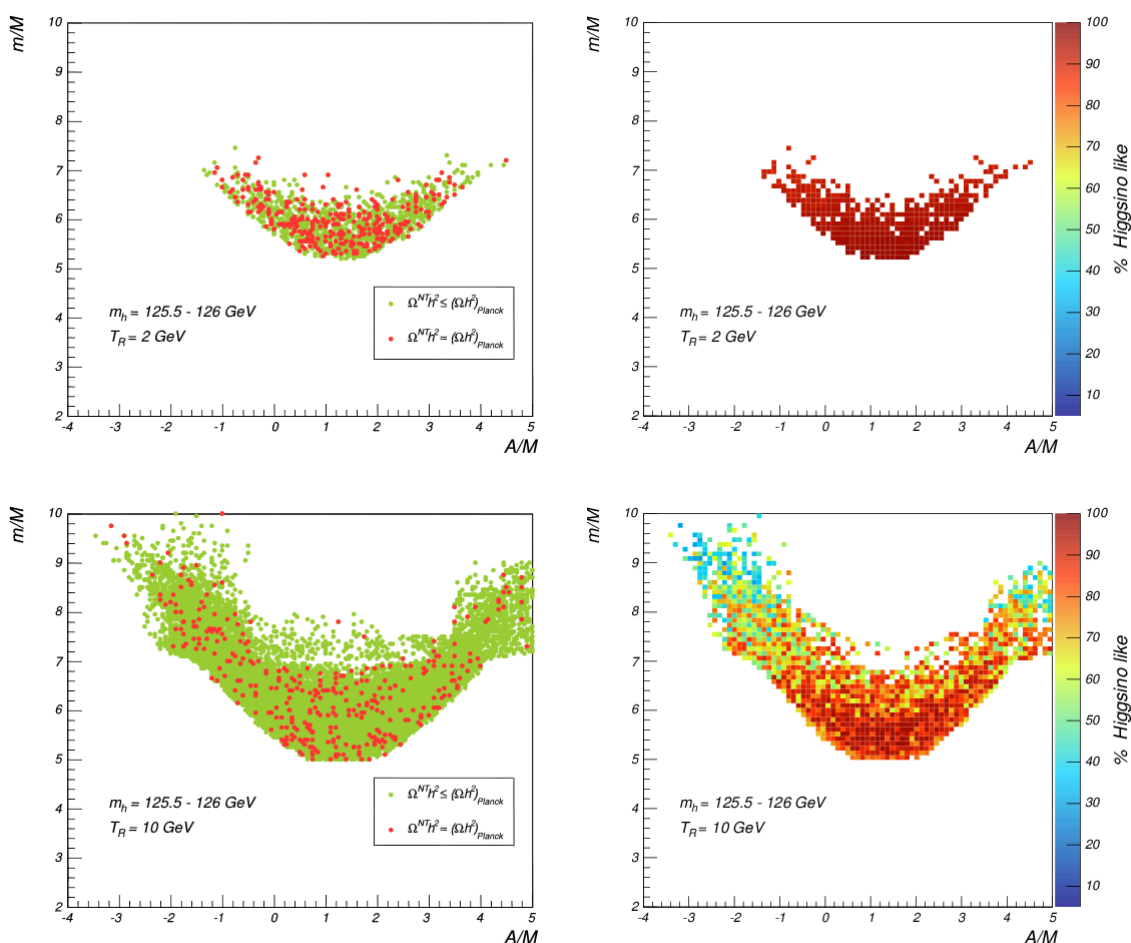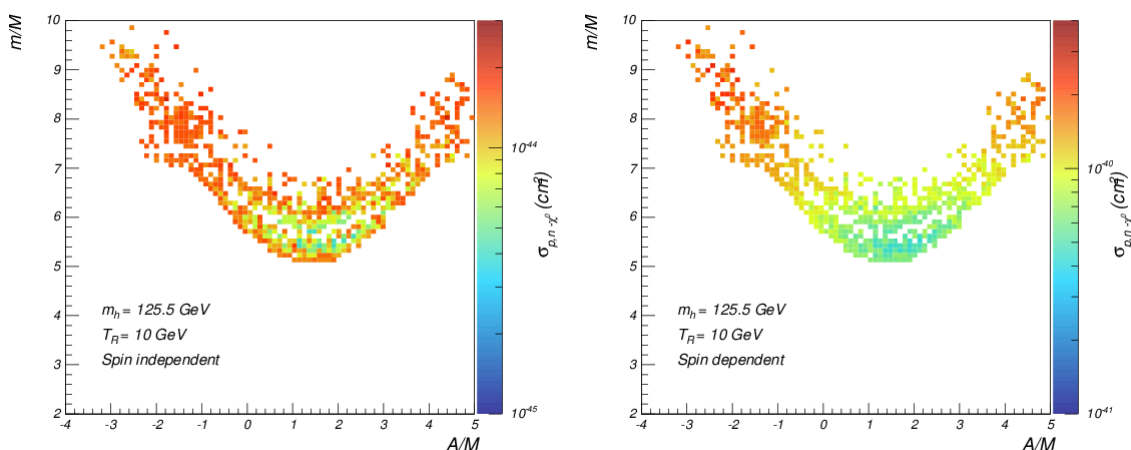
Figure 4. Case with $\mu > 0$: m/M vs A/M after imposing LEP, LHC, Planck and Fermi constraints (left) and corresponding LSP composition (right) for $m_h = 125.5$ - $126\,\mathrm{GeV}$ and $T_R = 2, 10\,\mathrm{GeV}$.

Figure 5 shows the spin independent and spin dependent WIMP-nucleon cross section after imposing LEP, LHC, Planck and Fermi constraints for $T_R = 10\,\mathrm{GeV}$. IceCube bounds rule out the orange and red regions of the right-hand side plot of figure 5.

Figure 6 shows the inclusion of LUX bounds on the spin independent direct detection constraints which rule out most of the points in figure 5 apart from a region corresponding to LSP masses around $300\,\mathrm{GeV}$ which is at the border of detectability.

Moreover, for $T_R = 2\,\mathrm{GeV}$ there are red points which saturate the observed DM content. In this case the neutralinos are becoming more pure Higgsinos in order to enhance the annihilation cross section and the Fermi constraint becomes harder to avoid but there are still regions allowed by both direct and indirect detection searches. There are more green points for $T_R = 10\,\mathrm{GeV}$ since the annihilation cross section becomes smaller due to Bino mixing which means a larger allowed region after using Fermi data but the constraint from the direct detection becomes more stringent (due to Bino-Higgsino mixing in the LSP) and

Figure 5. Case with $\mu > 0$: correlation between $a = m/M$ and $b = A/M$ after imposing LEP, LHC, Planck and Fermi (pass 8 limit) constraints with the corresponding spin independent (left) and spin dependent (right) WIMP-nucleon cross section for $m_h = 125.5 \, \text{GeV}$ and $T_R = 10 \, \text{GeV}$.
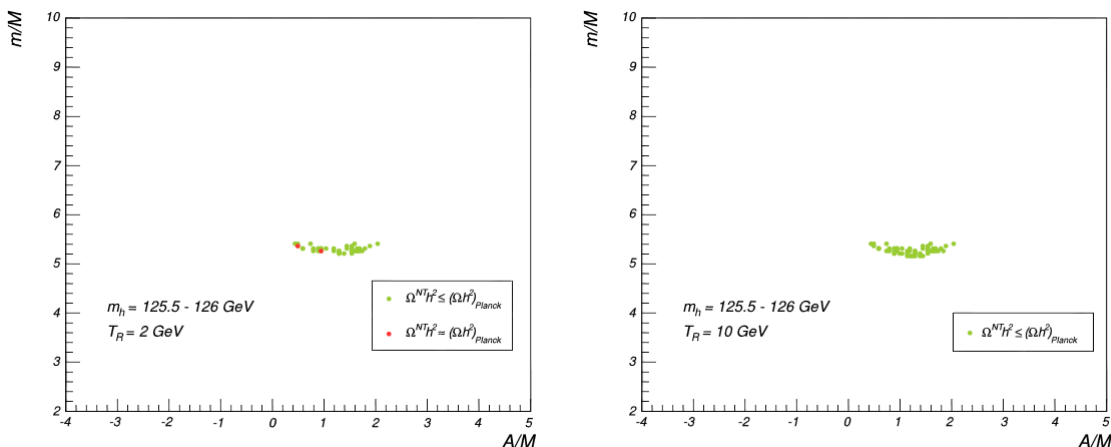

Figure 6. Case with $\mu > 0$: correlation between $a = m/M$ and $b = A/M$ after imposing LEP, LHC, Planck, Fermi and LUX bounds for $m_h = 125.5$ - $126 \, \text{GeV}$ and $T_R = 2, 10 \, \text{GeV}$.

so there are no red points which saturate the observed DM content.[6] For the points shown in figure 6, the GUT values $c = B/M$ and $d = \mu/M$ are around 0.6 and 1 respectively.

3.3.2 Results for negative μ

The results for the negative μ case are shown in figures 7 and 8. Note that under the same conditions the allowed parameter space for $\mu < 0$ is larger than the one for $\mu > 0$. This can be understood as follows [69, 70]: $\sigma_{\tilde{\chi}_1^0 - p}$ is dominated by the t-channel h, H exchange

---

[6]The direct detection exclusion however depends on various uncertainties, e.g. strange quark content of proton, form factor etc. [71–73].
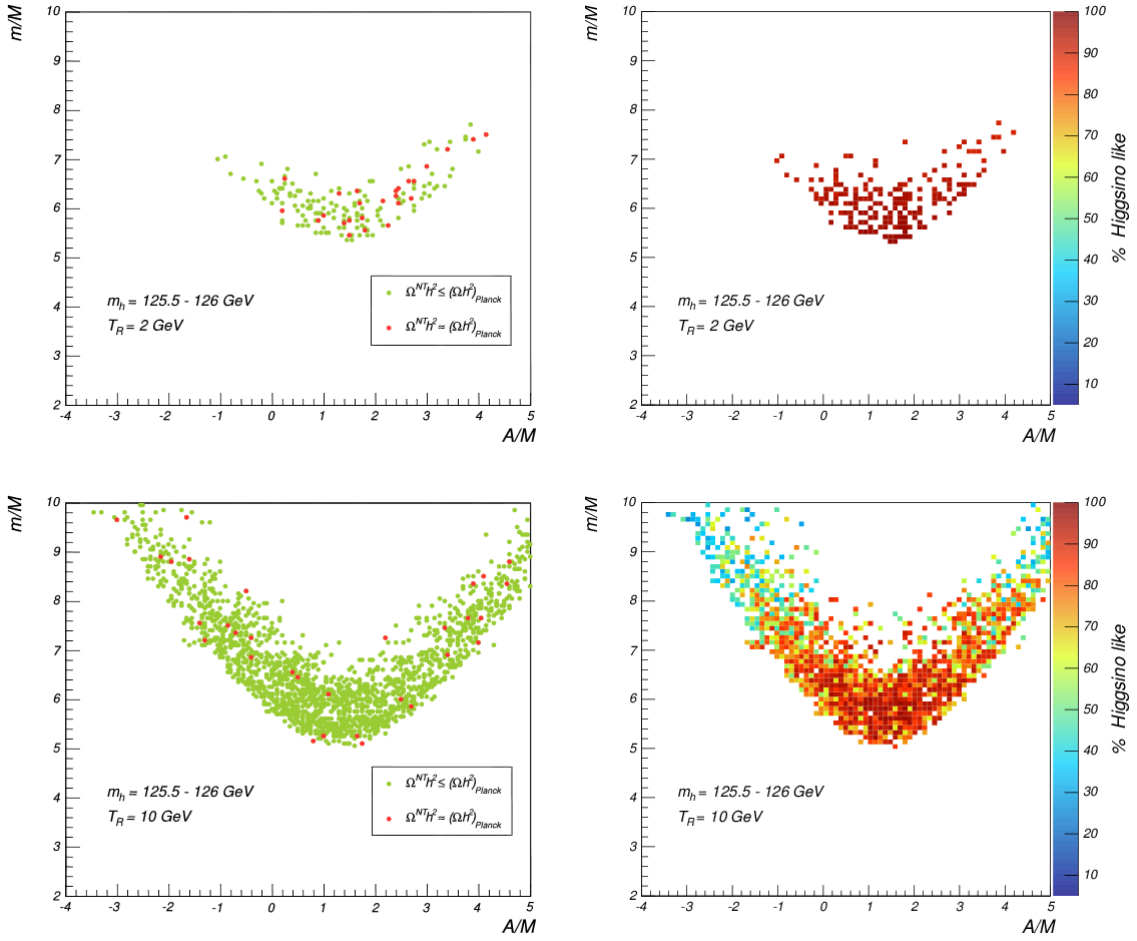
Figure 7. Case with $\mu < 0$: a versus b after imposing LEP, LHC, Planck and Fermi (pass 8 limit) bounds (left) and LSP composition (right) for $m_h = 125.5$ - $126\,\mathrm{GeV}$ and $T_R = 2, 10\,\mathrm{GeV}$.

diagrams which mostly arise from down type (s-quark) interaction:

$$A^d \propto m_d \left(\frac{\cos\alpha}{\cos\beta} \frac{F_H}{m_H^2} - \frac{\sin\alpha}{\cos\beta} \frac{F_h}{m_h^2} \right), \tag{3.8}$$

where α is the Higgs mixing angle, $F_h = (N_{12} - N_{11}\tan\theta_W)(N_{14}\cos\alpha + N_{13}\sin\alpha)$ and $F_H = (N_{12} - N_{11}\tan\theta_W)(N_{14}\sin\alpha - N_{13}\cos\alpha)$ using $\tilde{\chi}_1^0 = N_{11}\tilde{B} + N_{12}\tilde{W} + N_{13}\tilde{H}_1 + N_{14}\tilde{H}_2$. For $\mu < 0$, the ratio N_{14}/N_{13} is positive and this amplitude can become small due to cancellations if:

$$\frac{N_{14}}{N_{13}} = -\frac{\tan\alpha + m_h^2/m_H^2 \cot\alpha}{1 + m_h^2/m_H^2}, \tag{3.9}$$

is satisfied (for $\tan\alpha < 0$). In figure 8 there are more allowed points compared to figure 6 even if there are still no points which saturate the observed DM content for $T_R = 10\,\mathrm{GeV}$ due to stringent direct detection constraints. For the points shown in figure 8, the GUT scale values of B and μ are still both of order M.
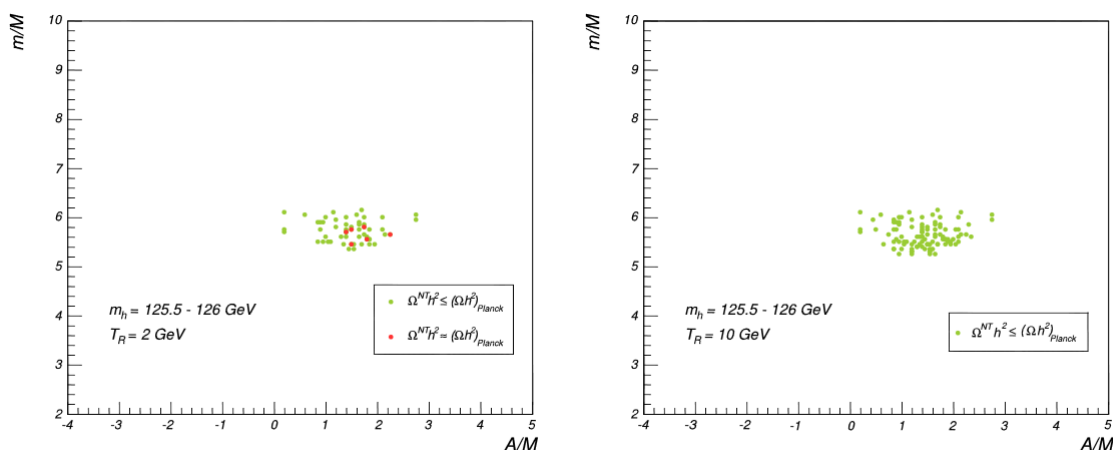
Figure 8. Case with $\mu < 0$: correlation between $a = m/M$ and $b = A/M$ after imposing LEP, LHC, Planck, Fermi (pass 8 limit) and LUX for $m_h = 125.5$ - $126\,\mathrm{GeV}$ and $T_R = 2, 10\,\mathrm{GeV}$.

4 Discussion of results

4.1 Analysis of the allowed parameter space

We are now in a position to put all our results together and explain the effect of each experimental bound on our parameter space. In the end we shall analyse the spectrum of superpartners that appears for the points surviving all the phenomenological constraints. All the observables analysed in this section have been computed numerically using `microOMEGAS` v3 [87] linked to `SPheno` v3.3.3 [85, 86].

Figure 9 shows the relation between the spin independent WIMP-nucleon cross section and the LSP mass. Depending on T_R there is a different upper bound for neutralino masses which is given by the Planck constraint on DM. For larger values of T_R, the non-thermal relic density decreases, and so heavier neutralinos can pass the Planck constraint on the DM relic density. On the other hand, for larger T_R the parameter space for standard thermal DM (orange band) becomes also larger. Note that LUX 2013 results exclude at 90% most of the parameter space and the next round of results (LUX 300 days) will be able to probe the remaining regions (the light blue points below the LUX line).

In the scenario we considered, the gaugino masses are unified at the GUT scale and therefore the evolution of electroweakinos is totally dominated by the RG flow. This implies that the LSP can only be Higgsino- or Bino-like (or a mixed combination of them). The largest contributions to the thermal averaged annihilation rates are given by (see for example [25] and references therein):

$$\langle \sigma_{\mathrm{eff}} v \rangle = \frac{g_2^4}{512\pi\mu^2} \left(21 + 3\tan^2\theta_W + 11\tan^4\theta_W \right),$$ (4.1)

for Higgsino-like neutralinos (in the limit $M_W \ll \mu$) annihilating into vector bosons through

chargino or neutralino interchange, and:

$$\langle \sigma_{\text{eff}} v \rangle = \sum_f \frac{g_2^4 \tan^2 \theta_W \left(T_{3_f} - Q_f \right)^4 r(1 + r^2)}{2\pi m_{\tilde{f}}^2 (1+r)^4} \,, \tag{4.2}$$

for Bino-like LSP annihilation into fermion-antifermion (T_{3_f} and Q_f are the third component of isospin and the fermion charge and $r = M_1^2/m_{\tilde{f}}^2$). This process is driven at tree level by the t-channel exchange of a slepton $\tilde{f}$. In the case where the LSP is a mixed composition of Higgsino and Bino, the expression of the annihilation rate is an interpolation between (4.1) and (4.2). Figure 9 shows also the effect of Fermi bounds. As suggested by (4.1) and (4.2), the most constrained regions are those with smaller LSP masses. The grey band corresponds to points excluded by LEP bounds on chargino direct production.

Figure 10 shows the amount of non-thermal DM relic density provided by the LSP in terms of its mass, together with the bounds from indirect detection and LUX. The Planck value of the DM content can be saturated in the region which is not ruled out by direct detection bounds only for $T_R = 2\,\text{GeV}$. Given that for larger T_R the amount of LSP DM gets smaller, the cases with $T_R > 2\,\text{GeV}$ require multi-component DM. Combining figure 9 and figure 10, we find that the LUX allowed regions, indirect detection limits and the abundance of LSP DM are correlated for different T_R. The allowed regions, where the observed DM content is saturated, depend on T_R but they are generically around $m_\chi \simeq 300\,\text{GeV}$.

In figure 11, we show the Planck constraints on indirect detection through DM annihilation during the recombination epoch. We use WW final states corresponding to an efficiency factor $f_{\text{eff}} = 0.2$ [74]. Even going all the way to the cosmic variance bound, these constraints turn out to be less stringent than those coming from Fermi and LUX. On the other hand, figure 11 shows the correlation between the LSP composition and the bounds coming from both direct and indirect detection. Concerning Fermi and Planck limits on DM annihilation, these bounds allow almost all possible combinations of Bino/Higgsino neutralinos. The restrictions coming from the $f\bar{f}$ and $W\bar{W}$ channels depend on the neutralino composition: for a Higgsino-like LSP, the most stringent constraint is due to annihilation into vector bosons, while for a Bino-like LSP the main constraint comes from annihilation into a fermion-antifermion pair.

The LUX constraints in figure 11 reduce the parameter space to the region where the LSP is mostly Higgsino-like. This could be a bit puzzling since the WIMP-nucleon cross section is dominated by the Higgs exchange channel:

$$\sigma_{\chi - p} \propto \frac{a_{\tilde{H}}^2 (g' a_{\tilde{B}} - g \, a_{\tilde{W}})^2}{m_h^4} \,, \tag{4.3}$$

where $a_{\tilde{H}}$, $a_{\tilde{B}}$ and $a_{\tilde{W}}$ are respectively the Higgsino, Bino and Wino LSP components. According to this expression, the cross section is enhanced when the Higgsino component increases. However in figure 11 direct detection bounds allow only points which are mainly Higgsino-like. The reason of this effect is in the effective coupling $\tilde{\chi}\tilde{\chi}h$ which for a Bino-like LSP looks like:

$$C_{\tilde{\chi}\tilde{\chi}h} \simeq \frac{m_Z \sin \theta_W \tan \theta_W}{M_1^2 - \mu^2} \left(M_1 + \mu \sin 2\beta \right), \tag{4.4}$$

– 14 –
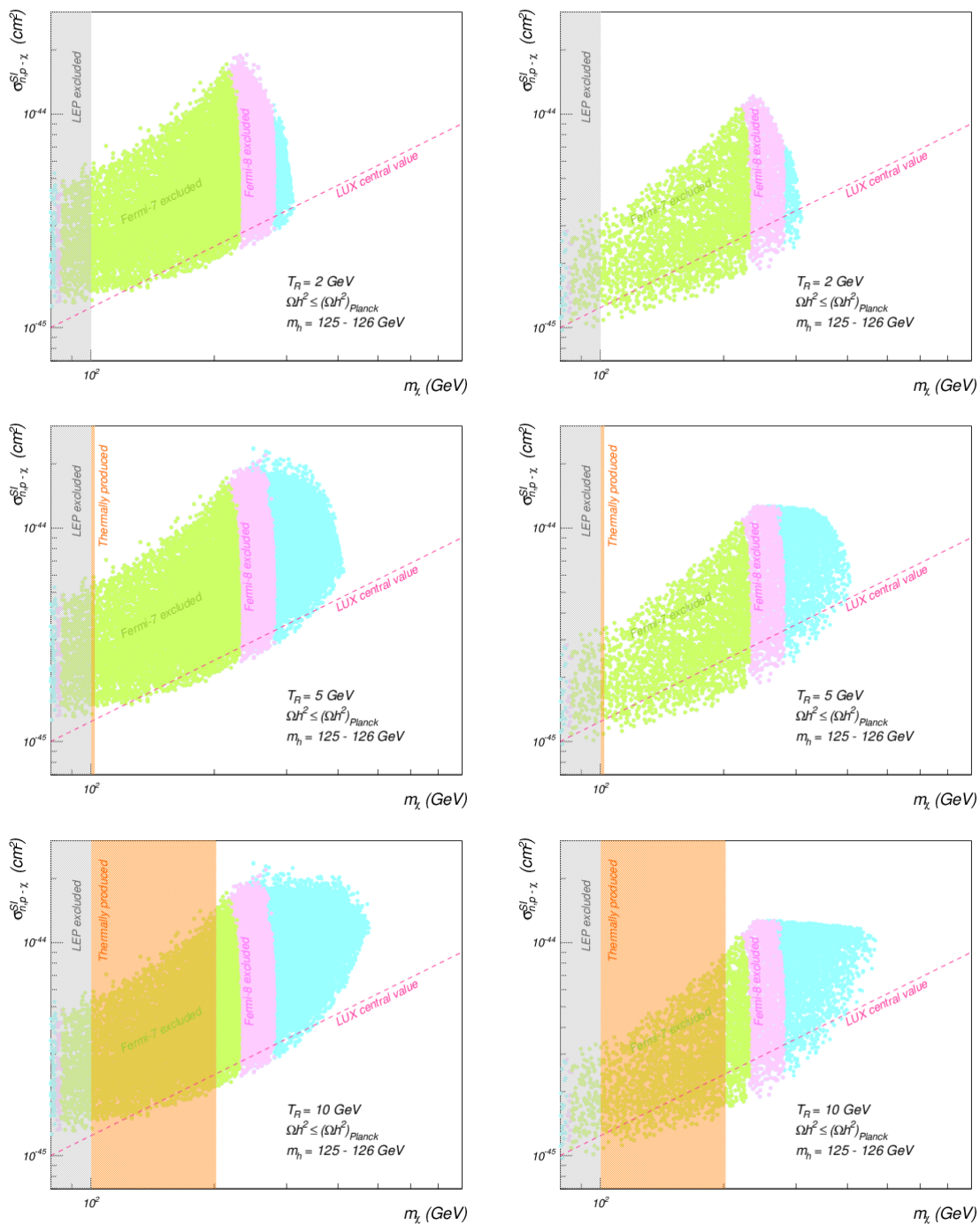
Figure 9. Spin independent cross section versus LSP mass for $\mu > 0$ (left) and $\mu < 0$ (right). The light blue points are not ruled out by indirect detection experiments. We show m_χ up to $800\,\mathrm{GeV}$.
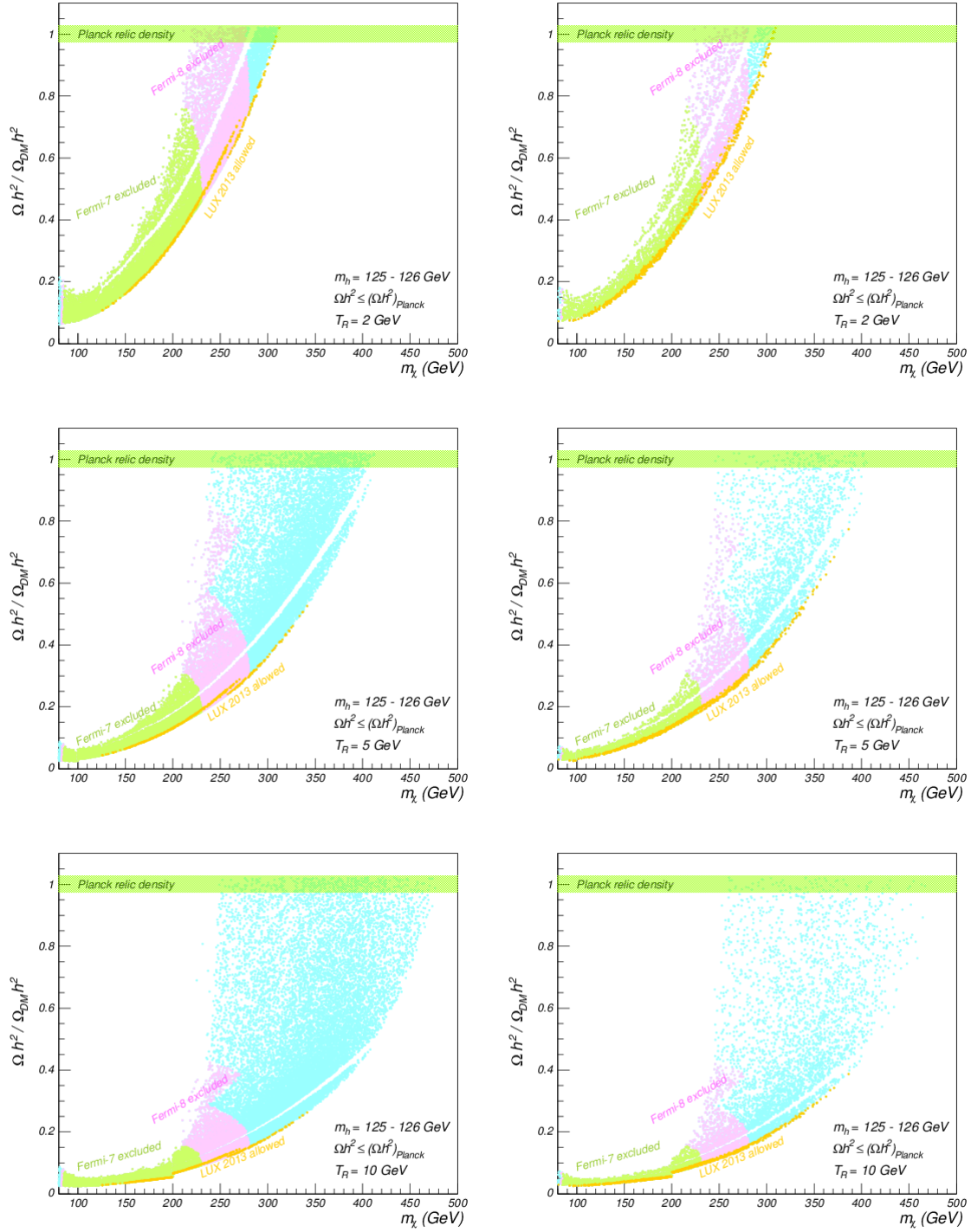
Figure 10. Non-thermal DM abundance predictions versus LSP mass for $\mu > 0$ (left) and $\mu < 0$ (right) and $T_R = 2, 5, 10 \, \text{GeV}$. The light blue points are not ruled out by indirect detection experiments while only the yellow points are allowed by LUX 2013 results.

where for moderate to large $\tan\beta$ the second term is negligible and $\mu > M_1$. Hence this coupling is dominated by M_1. On the other hand, the coupling for a Higgsino-like LSP is:

$$C_{\tilde{\chi}\tilde{\chi}h} \simeq \frac{1}{2}\left(1 \pm \sin 2\beta\right)\left(\tan^2\theta_W \frac{m_Z\cos\theta}{M_1 - |\mu|} + \frac{m_Z\cos\theta}{M_2 - |\mu|}\right), \tag{4.5}$$

where $\pm$ is for the H_u and H_d components and $\mu < M_1$. Contrary to the Bino-like case, this coupling is inversely proportional to M_1. Thus the WIMP-nucleon cross section grows in the regions where the LSP is Higgsino-like and M_1 is small or where the LSP is Bino-like and the gaugino mass is large. If we compare figure 2 (right) which shows the distribution of gaugino masses along the V-shaped band, with figure 4 (right) and 7 (right), we realise that the region with a smaller cross section is the one at the bottom of the V-shaped band where gaugino masses are big and the LSP is very Higgsino-like. The region where the LSP is more Bino-like has smaller gaugino masses and the cross section is larger. Fermi constraints however become more stringent in the case with more Higgsino content due to larger annihilation cross section. The competition between LUX and Fermi constraints produces the allowed parameter space where the Planck value of the DM content is saturated for $T_R = 2\,\text{GeV}$.

Finally, in figure 11 there is a change of behaviour of the thermal averaged cross section for masses around $130\,\text{GeV}$. The reason is the following: this region is (as can be shown in the plot) Higgsino-like, but the masses are closer to M_W and $\langle\sigma v\rangle$ is no longer described by (4.1) but by something like (with $x = \mu/m_W$):

$$\langle\sigma_{\text{eff}}v\rangle \sim \frac{9g^4}{16\pi m_W^2}\frac{x^2}{(4x^2 - 1)^2}. \tag{4.6}$$

In figure 12, we show the spectra of SUSY particles for the allowed regions of figure 6 (blue points below the LUX line). We find that sleptons, staus, Higgses, all other scalar masses and gluinos are rather heavy since they are between about 2 and $7\,\text{TeV}$. The lightest and second to lightest neutralino and the lightest chargino are around 280 - $340\,\text{GeV}$ while all other neutralinos and charginos are heavy. The allowed region for $T_R = 2\,\text{GeV}$ is shown on the left side of the vertical line with the label $T_R = 2\,\text{GeV}$ where the points situated exactly on the line satisfy all the constraints including the current DM content as measured by Planck. Similarly, the allowed region for $T_R \geq 5\,\text{GeV}$ is shown on the left side of the vertical line with the label $T_R \geq 5\,\text{GeV}$ even if there are no points in this region which saturate the current DM content. Notice that the spectrum is essentially independent of the reheating temperature T_R and the hierarchy between the different sparticles is robust.

4.2 Astrophysical uncertainties

The direct detection cross section can involve various uncertainties, e.g. strange quark content of proton, form factor, local DM density and LSP contribution to the total amount of observed DM abundance. The local density can be 0.1-0.7 GeV/cm^3 [75]. There could also be astrophysical uncertainties in the indirect detection results beyond what has been considered so far. Recently, it is mentioned in [76, 77] that if the thermal neutralinos do not produce the entire amount of cold dark matter, the direct and indirect detection
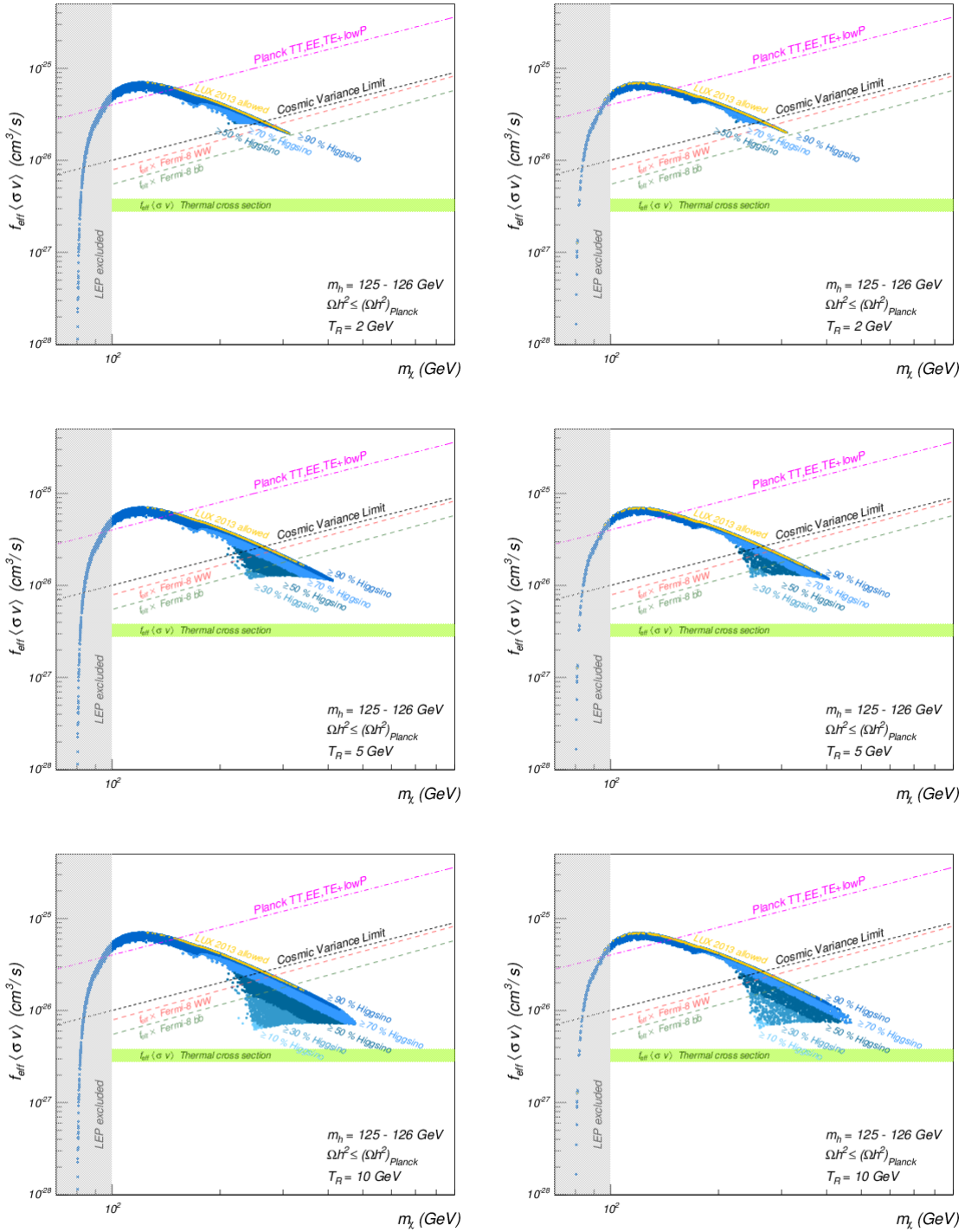
Figure 11. Comparison between detection constraints from Planck, Fermi and LUX for $\mu > 0$ (left) and $\mu < 0$ (right). We have set $f_{\text{eff}} = 0.2$. We show m_χ up to $900\,\text{GeV}$.

cross sections should be reduced by R and R^2 respectively with $R \equiv \Omega h^2/0.12$. Possible bounds arising from Fermi are now almost negligible since they are suppressed by R^2.
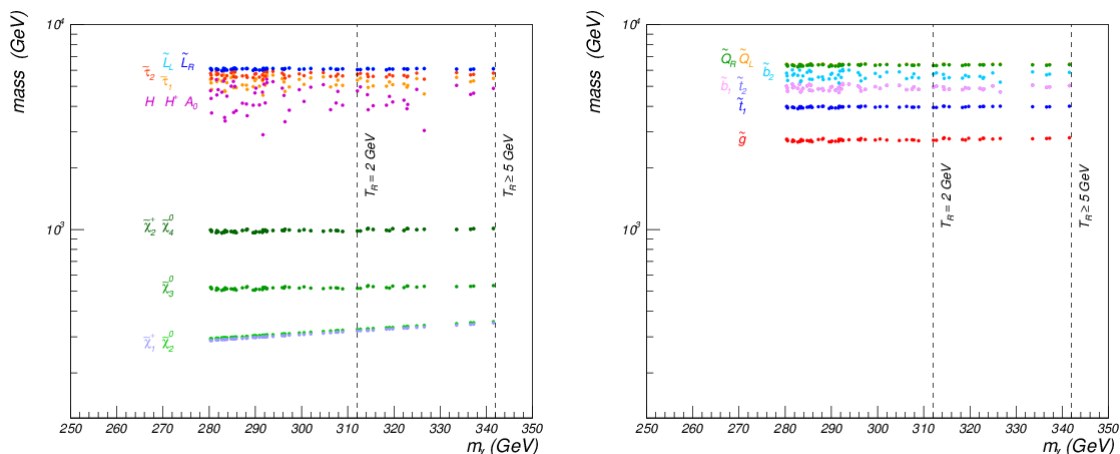
Figure 12. The mass spectra of superpartners for allowed points shown in figure 6 for different values of T_R.

Once the suppression factor R is taken into account, Fermi, Planck and other indirect detection experiments have lower impacts. Concerning the effect on LUX and other direct detection bounds, the cross section is now reduced by R which is equivalent to multiplying the effective couplings (4.4) and (4.5) by $\sqrt{R}$. This clearly introduces a new parameter in the discussion performed in the previous section.

If we assume such a reduction in the cases where $\Omega^{NT}h^2 \leq 0.12$, more parameter space could be allowed for multi-component DM regions as shown in figure 13. The pink region is disallowed by Fermi data. The T_R dependence of the region constrained by Fermi in figure 13 is due to the fact that the factor R is now a function of T_R

$$R = \frac{\Omega^{NT}h^2}{0.12} \simeq \frac{T_f}{T_R}\frac{\Omega^{Th}h^2}{0.12}. \tag{4.7}$$

R becomes larger for smaller values of T_R $(=2\,\text{GeV})$ and the Fermi constraint becomes important.

The region below the dashed line satisfied present LUX limits. In particular this implies that the region with lighter neutralinos is now unconstrained by LUX. This region typically corresponds to more Bino component in the LSP as shown in figure 4 (right) and 7 (right). We have therefore a different situation compared to before, because now neutralinos with a larger Bino component are allowed.

Let us stress, however, that the prediction for the region where $\Omega^{NT}h^2$ saturates the DM content remains unchanged, i.e. only the case $T_R = 2\,\text{GeV}$ contains points which are still allowed by all data and saturate the DM content with an LSP mass around $300\,\text{GeV}$.

This new factor R helps us to extract more parameter space for the multi-component DM scenarios. However, the DM simulations need to establish the validity of the assumption that proportions of various DM components in the early universe is maintained even after the large scale structures are formed.
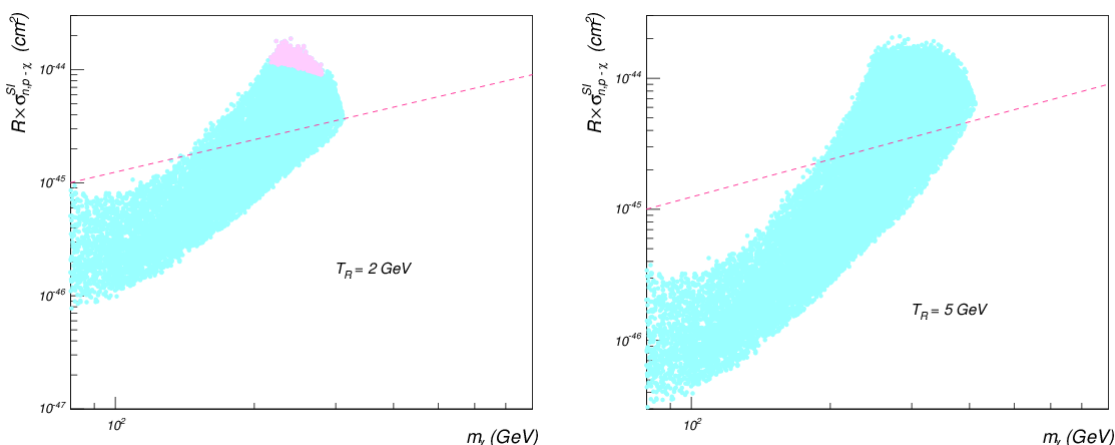
Figure 13. $R \times \sigma^{SI}_{n,p-\tilde{\chi}^0_1}$ vs $m_{\tilde{\chi}^0_1}$ for $T_R = 2, 5 \, \text{GeV}$. R is defined in the text. More parameter space is allowed.

5 Conclusions

Non-thermal DM scenarios emerge in UV theories like string theory due to the presence of gravitationally coupled scalars which decay at late times when they are dominating the energy density of the universe. In such models the reheating temperature due to moduli decays is typically below the freeze-out temperature, $T_R < T_f$ when assuming an MSSM particle as main DM constituent. In this paper, we have studied the non-thermal version of the CMSSM/mSUGRA and contrasted it with both particle physics and astrophysical experimental constraints. The experimental information available at this moment, including the well known value of the Higgs mass, is enough to rule out the vast majority of the non-thermal CMSSM parameter space. There is still a small region which is consistent with all observations and is at the edge of detection by both astrophysics and particle physics experiments, resulting in a very interesting situation for beyond the SM physics.

In our determination of the allowed parameter space we have used constraints from collider experiments (LEP, LHC), cosmic microwave background observations (Planck) and direct and indirect DM searches (Fermi, XENON100, IceCube, LUX, CDMS). We have found that the most restrictive constraints come from Fermi and LUX which single out a small region of the non-thermal CMSSM parameter space corresponding to a Higgsino-like LSP with a mass around $300 \, \text{GeV}$ that can saturate the observed DM abundance for $T_R \simeq 2 \, \text{GeV}$ while larger reheating temperatures require additional contributions to the present DM abundance. These results are summarised in figure 10 which shows the comparison between the cases of positive and negative μ.

This non-thermal scenario leads to a clear pattern of SUSY particles. In particular, the fact that the LSP is Higgsino-like makes the lightest chargino, the lightest neutralino and next to lightest neutralino to be almost degenerate in mass. This kind of scenario can be probed at the LHC using monojet plus soft leptons plus missing energy [78, 79], monojet

signal [80] and two Vector Boson Fusion jets and large missing transverse energy [81]. On the other hand, all the other superpartners are much heavier and beyond the LHC reach but accessible to potential future experiments such as a 100 TeV machine.

It is worth mentioning that non-thermal CMSSM scenarios with TeV-scale soft terms and reheating temperatures around 1 - 10 GeV can emerge in string models where the visible sector is sequestered from the sources of SUSY breaking [21, 22]. In a subset of the parameter range these string scenarios lead to $M_{\mathrm{soft}} \sim M_P \epsilon^2 \ll m_{\mathrm{mod}} \sim M_P \epsilon^{3/2} \ll M_{\mathrm{GUT}} \sim M_P \epsilon^{1/3}$ and $T_R \sim M_P \epsilon^{9/4}$ where $\epsilon \simeq m_{3/2}/M_P \ll 1$. For $\epsilon \sim 10^{-8}$, one obtains TeV-scale soft terms, $M_{\mathrm{GUT}} \sim 10^{16}\,\mathrm{GeV}$, $T_R \sim 1 - 10\,\mathrm{GeV}$ and $m_{\mathrm{mod}} \sim 10^6\,\mathrm{GeV}$ for $m_{3/2} \sim 10^{10}\,\mathrm{GeV}$.

We point out that our analysis is based on the CMSSM/mSUGRA for which all superpartners are expected to be at similar masses close to the TeV scale. In this sense we restricted ourselves to scalar masses lighter than 5 TeV which is the range of validity of the codes we have used to perform our analysis. There are however several ways to generalise this simplest scenario:

- Consider non-universal extensions of the CMSSM. Small departures from universality, even though strongly constrained by flavour changing neutral currents, allow more flexibility in the parameter space and will slightly enhance the allowed region.

- Consider sfermions heavier than 5 TeV as in the split SUSY case. This is not only an interesting phenomenological possibility but is also the other class of scenarios that were derived in the string compactifications studied in [21, 22].

- Consider MSSM scenarios with R-parity violation and late decaying moduli fields. This class of models has not been studied in detail and given the fact that even with R-parity conservation there seems to be a need for other sources of DM such as axions or axinos, this should be a possibility worth studying.

- Consider explicit D-brane models which tend to generate models beyond the standard MSSM (see for instance [82–84] for such models).

It is encouraging that new planned experiments such as upcoming LUX result and XENON1T will be enough to rule out the rest of the allowed parameter space, independent of the upcoming LHC run. Clearly also new LHC runs and future planned colliders will be crucial for this class of models. Combining astrophysical and collider measurements is probably the most efficient way to constrain beyond the SM physics and this article is a clear illustration of this strategy.

Acknowledgments

References

[1] J.D. Barrow, *Massive Particles As A Probe Of The Early Universe*, [*Nucl. Phys.* **B 208** (1982) 501](#) [ɪɴSPIRE].

[2] M. Kamionkowski and M.S. Turner, *Thermal Relics: Do We Know Their Abundances?*, [*Phys. Rev.* **D 42** (1990) 3310](#) [ɪɴSPIRE].

[3] T. Moroi and L. Randall, *Wino cold dark matter from anomaly mediated SUSY breaking*, [*Nucl. Phys.* **B 570** (2000) 455](#) [`hep-ph/9906527`] [ɪɴSPIRE].

[4] M. Fujii and K. Hamaguchi, *Higgsino and wino dark matter from Q ball decay*, [*Phys. Lett.* **B 525** (2002) 143](#) [`hep-ph/0110072`] [ɪɴSPIRE].

[5] R. Kitano, H. Murayama and M. Ratz, *Unified origin of baryons and dark matter*, [*Phys. Lett.* **B 669** (2008) 145](#) [`arXiv:0807.4313`] [ɪɴSPIRE].

[6] B. Dutta, L. Leblond and K. Sinha, *Mirage in the Sky: Non-thermal Dark Matter, Gravitino Problem and Cosmic Ray Anomalies*, [*Phys. Rev.* **D 80** (2009) 035014](#) [`arXiv:0904.3773`] [ɪɴSPIRE].

[7] G.D. Coughlan, W. Fischler, E.W. Kolb, S. Raby and G.G. Ross, *Cosmological Problems for the Polonyi Potential*, [*Phys. Lett.* **B 131** (1983) 59](#) [ɪɴSPIRE].

[8] T. Banks, D.B. Kaplan and A.E. Nelson, *Cosmological implications of dynamical supersymmetry breaking*, [*Phys. Rev.* **D 49** (1994) 779](#) [`hep-ph/9308292`] [ɪɴSPIRE].

[9] B. de Carlos, J.A. Casas, F. Quevedo and E. Roulet, *Model independent properties and cosmological implications of the dilaton and moduli sectors of $4 - D$ strings*, [*Phys. Lett.* **B 318** (1993) 447](#) [`hep-ph/9308325`] [ɪɴSPIRE].

[10] B.S. Acharya et al., *Non-thermal Dark Matter and the Moduli Problem in String Frameworks*, [*JHEP* **06** (2008) 064](#) [`arXiv:0804.0863`] [ɪɴSPIRE].

[11] B.S. Acharya, G. Kane, S. Watson and P. Kumar, *A Non-thermal WIMP Miracle*, [*Phys. Rev.* **D 80** (2009) 083529](#) [`arXiv:0908.2430`] [ɪɴSPIRE].

[12] B.S. Acharya, G. Kane and E. Kuflik, *Bounds on scalar masses in theories of moduli stabilization*, [*Int. J. Mod. Phys.* **A 29** (2014) 1450073](#) [`arXiv:1006.3272`] [ɪɴSPIRE].

[13] R. Allahverdi, M. Cicoli, B. Dutta and K. Sinha, *Nonthermal dark matter in string compactifications*, [*Phys. Rev.* **D 88** (2013) 095015](#) [`arXiv:1307.5086`] [ɪɴSPIRE].

[14] M. Dine, L. Randall and S.D. Thomas, *Baryogenesis from flat directions of the supersymmetric standard model*, [*Nucl. Phys.* **B 458** (1996) 291](#) [`hep-ph/9507453`] [ɪɴSPIRE].

[15] W. Buchmüller, K. Hamaguchi, O. Lebedev and M. Ratz, *Maximal temperature in flux compactifications*, [*JCAP* **01** (2005) 004](#) [`hep-th/0411109`] [ɪɴSPIRE].

[16] L. Anguelova, V. Calo and M. Cicoli, *LARGE Volume String Compactifications at Finite Temperature*, *JCAP* **10** (2009) 025 [arXiv:0904.0051] [INSPIRE].

[17] K. Choi, A. Falkowski, H.P. Nilles and M. Olechowski, *Soft supersymmetry breaking in KKLT flux compactification*, *Nucl. Phys.* **B 718** (2005) 113 [hep-th/0503216] [INSPIRE].

[18] V. Lowen and H.P. Nilles, *Mirage Pattern from the Heterotic String*, *Phys. Rev.* **D 77** (2008) 106007 [arXiv:0802.1137] [INSPIRE].

[19] B.S. Acharya, K. Bobkov, G.L. Kane, J. Shao and P. Kumar, *The G_2-MSSM: An M-theory motivated model of Particle Physics*, *Phys. Rev.* **D 78** (2008) 065038 [arXiv:0801.0478] [INSPIRE].

[20] E. Dudas, A. Linde, Y. Mambrini, A. Mustafayev and K.A. Olive, *Strong moduli stabilization and phenomenology*, *Eur. Phys. J.* **C 73** (2013) 2268 [arXiv:1209.0499] [INSPIRE].

[21] R. Blumenhagen, J.P. Conlon, S. Krippendorf, S. Moster and F. Quevedo, *SUSY Breaking in Local String/F-Theory Models*, *JHEP* **09** (2009) 007 [arXiv:0906.3297] [INSPIRE].

[22] L. Aparicio et al., *Sequestered de Sitter String Scenarios: Soft-terms*, *JHEP* **11** (2014) 071 [arXiv:1409.1931] [INSPIRE].

[23] H. Baer, V. Barger and A. Mustafayev, *Neutralino dark matter in mSUGRA/CMSSM with a 125 GeV light Higgs scalar*, *JHEP* **05** (2012) 091 [arXiv:1202.4038] [INSPIRE].

[24] S. Krippendorf, H.P. Nilles, M. Ratz and M.W. Winkler, *Hidden SUSY from precision gauge unification*, *Phys. Rev.* **D 88** (2013) 035022 [arXiv:1306.0574] [INSPIRE].

[25] N. Arkani-Hamed, A. Delgado and G.F. Giudice, *The Well-tempered neutralino*, *Nucl. Phys.* **B 741** (2006) 108 [hep-ph/0601041] [INSPIRE].

[26] R.L. Arnowitt and P. Nath, *SUSY mass spectrum in* SU(5) *supergravity grand unification*, *Phys. Rev. Lett.* **69** (1992) 725 [INSPIRE].

[27] V.D. Barger, M.S. Berger and P. Ohmann, *The Supersymmetric particle spectrum*, *Phys. Rev.* **D 49** (1994) 4908 [hep-ph/9311269] [INSPIRE].

[28] G.L. Kane, C.F. Kolda, L. Roszkowski and J.D. Wells, *Study of constrained minimal supersymmetry*, *Phys. Rev.* **D 49** (1994) 6173 [hep-ph/9312272] [INSPIRE].

[29] H. Baer and M. Brhlik, *QCD improved $b \to s\gamma$ constraints on the minimal supergravity model*, *Phys. Rev.* **D 55** (1997) 3201 [hep-ph/9610224] [INSPIRE].

[30] LEP2 SUSY Working Group, *Combined LEP Selectron/Smuon/Stau Results*, 183-208 GeV (2004), note LEPSUSYWG/04-01.1, http://lepsusy.web.cern.ch/lepsusy/.

[31] LEP2 SUSY Working Group, *Combined LEP Chargino Results, up to 208 GeV for large m0*, note LEPSUSYWG/01-03.1', http://lepsusy.web.cern.ch/lepsusy/.

[32] LEP2 SUSY Working Group, *Combined LEP Chargino Results, up to 208 GeV for low DM*, note LEPSUSYWG/02-04.1, http://lepsusy.web.cern.ch/lepsusy/.

[33] LEP2 SUSY Working Group, *Combined Lower Bound of the Neutralino Mass in a Constrained MSSM model*, note LEPSUSYWG/04-07.1, http://lepsusy.web.cern.ch/lepsusy/.

[34] ATLAS collaboration, *Search for squarks and gluinos with the ATLAS detector in final states with jets and missing transverse momentum using $\sqrt{s} = 8$ TeV proton-proton collision data*, CERN-PH-EP-2014-093 (2014).

[35] ATLAS collaboration, *Hunt for new phenomena using large jet multiplicities and missing transverse momentum with ATLAS in 4.7 fb^{-1} of $\sqrt{s} = 7$ TeV proton-proton collisions*, *JHEP* **07** (2012) 167 [arXiv:1206.1760] [INSPIRE].

[36] CMS collaboration, *Search for new physics in the multijet and missing transverse momentum final state in proton-proton collisions at $\sqrt{s} = 7$ TeV*, *Phys. Rev. Lett.* **109** (2012) 171803 [arXiv:1207.1898] [INSPIRE].

[37] CMS collaboration, *Search for new physics in the multijet and missing transverse momentum final state in proton-proton collisions at $\sqrt{s} = 7$ TeV*, *Phys. Rev. Lett.* **109** (2012) 171803 [arXiv:1207.1898] [INSPIRE].

[38] ATLAS collaboration, *Search for direct production of charginos, neutralinos and sleptons in final states with two leptons and missing transverse momentum in pp collisions at $\sqrt{s} = 8$ TeV with the ATLAS detector*, *JHEP* **05** (2014) 071 [arXiv:1403.5294] [INSPIRE].

[39] CMS collaboration, *Searches for electroweak production of charginos, neutralinos and sleptons decaying to leptons and W, Z and Higgs bosons in pp collisions at 8 TeV*, *Eur. Phys. J.* **C 74** (2014) 3036 [arXiv:1405.7570] [INSPIRE].

[40] PLANCK collaboration, P.A.R. Ade et al., *Planck 2015 results. XIII. Cosmological parameters*, arXiv:1502.01589 [INSPIRE].

[41] FERMI-LAT collaboration, M. Ackermann et al., *Limits on Dark Matter Annihilation Signals from the Fermi LAT 4-year Measurement of the Isotropic Gamma-Ray Background*, arXiv:1501.05464 [INSPIRE].

[42] XENON collaboration, S.E.A. Orrigo, *Direct Dark Matter Search with XENON100*, arXiv:1501.03492 [INSPIRE].

[43] CDMS collaboration, R. Agnese et al., *Silicon Detector Dark Matter Results from the Final Exposure of CDMS II*, *Phys. Rev. Lett.* **111** (2013) 251301 [arXiv:1304.4279] [INSPIRE].

[44] ICECUBE collaboration, M.G. Aartsen et al., *Search for dark matter annihilations in the Sun with the 79-string IceCube detector*, *Phys. Rev. Lett.* **110** (2013) 131302 [arXiv:1212.4097] [INSPIRE].

[45] LUX collaboration, D.S. Akerib et al., *First results from the LUX dark matter experiment at the Sanford Underground Research Facility*, *Phys. Rev. Lett.* **112** (2014) 091303 [arXiv:1310.8214] [INSPIRE].

[46] R. Allahverdi, M. Cicoli, B. Dutta and K. Sinha, *Correlation between Dark Matter and Dark Radiation in String Compactifications*, *JCAP* **10** (2014) 002 [arXiv:1401.4364] [INSPIRE].

[47] M. Cicoli, C. Mayrhofer and R. Valandro, *Moduli Stabilisation for Chiral Global Models*, *JHEP* **02** (2012) 062 [arXiv:1110.3333] [INSPIRE].

[48] M. Cicoli, S. Krippendorf, C. Mayrhofer, F. Quevedo and R. Valandro, *D-Branes at del Pezzo Singularities: Global Embedding and Moduli Stabilisation*, *JHEP* **09** (2012) 019 [arXiv:1206.5237] [INSPIRE].

[49] M. Cicoli et al., *Explicit de Sitter Flux Vacua for Global String Models with Chiral Matter*, *JHEP* **05** (2014) 001 [arXiv:1312.0014] [INSPIRE].

[50] J.P. Conlon and F. Quevedo, *Kähler moduli inflation*, *JHEP* **01** (2006) 146 [hep-th/0509012] [INSPIRE].

[51] C.P. Burgess, M. Cicoli and F. Quevedo, *String Inflation After Planck 2013*, *JCAP* **11** (2013) 003 [arXiv:1306.3512] [INSPIRE].

[52] M. Cicoli and F. Quevedo, *String moduli inflation: An overview*, *Class. Quant. Grav.* **28** (2011) 204001 [arXiv:1108.2659] [INSPIRE].

[53] K. Dutta and A. Maharana, *Inflationary constraints on modulus dominated cosmology*, *Phys. Rev.* **D 91** (2015) 043503 [arXiv:1409.7037] [INSPIRE].

[54] M. Endo, K. Hamaguchi and F. Takahashi, *Moduli-induced gravitino problem*, *Phys. Rev. Lett.* **96** (2006) 211301 [hep-ph/0602061] [INSPIRE].

[55] S. Nakamura and M. Yamaguchi, *Gravitino production from heavy moduli decay and cosmological moduli problem revived*, *Phys. Lett.* **B 638** (2006) 389 [hep-ph/0602081] [INSPIRE].

[56] L. Roszkowski, S. Trojanowski and K. Turzynski, *Neutralino and gravitino dark matter with low reheating temperature*, *JHEP* **11** (2014) 146 [arXiv:1406.0012] [INSPIRE].

[57] T. Cohen, M. Lisanti, A. Pierce and T.R. Slatyer, *Wino Dark Matter Under Siege*, *JCAP* **10** (2013) 061 [arXiv:1307.4082] [INSPIRE].

[58] R. Allahverdi, B. Dutta and K. Sinha, *Baryogenesis and Late-Decaying Moduli*, *Phys. Rev.* **D 82** (2010) 035004 [arXiv:1005.2804] [INSPIRE].

[59] R. Allahverdi, B. Dutta and K. Sinha, *Cladogenesis: Baryon-Dark Matter Coincidence from Branchings in Moduli Decay*, *Phys. Rev.* **D 83** (2011) 083502 [arXiv:1011.1286] [INSPIRE].

[60] R. Allahverdi, B. Dutta and K. Sinha, *Non-thermal Higgsino Dark Matter: Cosmological Motivations and Implications for a 125 GeV Higgs*, *Phys. Rev.* **D 86** (2012) 095016 [arXiv:1208.0115] [INSPIRE].

[61] R. Allahverdi, B. Dutta and K. Sinha, *Successful Supersymmetric Dark Matter with Thermal Over/Under-Abundance from Late Decay of a Visible Sector Scalar*, *Phys. Rev.* **D 87** (2013) 075024 [arXiv:1212.6948] [INSPIRE].

[62] R. Allahverdi, B. Dutta, R.N. Mohapatra and K. Sinha, *A Supersymmetric Model for Dark Matter and Baryogenesis Motivated by the Recent CDMS Result*, *Phys. Rev. Lett.* **111** (2013) 051302 [arXiv:1305.0287] [INSPIRE].

[63] M. Cicoli, J.P. Conlon and F. Quevedo, *Dark radiation in LARGE volume models*, *Phys. Rev.* **D 87** (2013) 043520 [arXiv:1208.3562] [INSPIRE].

[64] T. Higaki and F. Takahashi, *Dark Radiation and Dark Matter in Large Volume Compactifications*, *JHEP* **11** (2012) 125 [arXiv:1208.3563] [INSPIRE].

[65] CMS, LHCb collaboration, *Observation of the rare $B_s^0 \to \mu^+\mu^-$ decay from the combined analysis of CMS and LHCb data*, arXiv:1411.4413 [INSPIRE].

[66] Particle Data Group collaboration, K.A. Olive et al., *Review of Particle Physics*, *Chin. Phys.* **C 38** (2014) 090001.

[67] J.L. Feng, K.T. Matchev and T. Moroi, *Focus points and naturalness in supersymmetry*, *Phys. Rev.* **D 61** (2000) 075005 [hep-ph/9909334] [INSPIRE].

[68] M. Carena, J.R. Espinosa, M. Quirós and C.E.M. Wagner, *Analytical expressions for radiatively corrected Higgs masses and couplings in the MSSM*, *Phys. Lett.* **B 355** (1995) 209 [hep-ph/9504316] [INSPIRE].

[69] R.L. Arnowitt, B. Dutta and Y. Santoso, *Coannihilation effects in supergravity and D-brane models*, *Nucl. Phys.* **B 606** (2001) 59 [hep-ph/0102181] [INSPIRE].

[70] J.R. Ellis, A. Ferstl and K.A. Olive, *Exploration of elastic scattering rates for supersymmetric dark matter*, *Phys. Rev.* **D 63** (2001) 065016 [hep-ph/0007113] [INSPIRE].

[71] E. Accomando, R.L. Arnowitt, B. Dutta and Y. Santoso, *Neutralino proton cross-sections in supergravity models*, *Nucl. Phys.* **B 585** (2000) 124 [hep-ph/0001019] [INSPIRE].

[72] A. Bottino, F. Donato, N. Fornengo and S. Scopel, *Implications for relic neutralinos of the theoretical uncertainties in the neutralino nucleon cross-section*, *Astropart. Phys.* **13** (2000) 215 [hep-ph/9909228] [INSPIRE].

[73] J.R. Ellis, K.A. Olive and C. Savage, *Hadronic Uncertainties in the Elastic Scattering of Supersymmetric Dark Matter*, *Phys. Rev.* **D 77** (2008) 065026 [arXiv:0801.3656] [INSPIRE].

[74] M.S. Madhavacheril, N. Sehgal and T.R. Slatyer, *Current Dark Matter Annihilation Constraints from CMB and Low-Redshift Data*, *Phys. Rev.* **D 89** (2014) 103508 [arXiv:1310.3815] [INSPIRE].

[75] J.I. Read, *The Local Dark Matter Density*, *J. Phys.* **G 41** (2014) 063101 [arXiv:1404.1938] [INSPIRE].

[76] H. Baer et al., *Natural SUSY with a bino- or wino-like LSP*, *Phys. Rev.* **D 91** (2015) 075005 [arXiv:1501.06357] [INSPIRE].

[77] M. Cahill-Rowley et al., *Complementarity and Searches for Dark Matter in the pMSSM*, arXiv:1305.6921 [INSPIRE].

[78] H. Baer, A. Mustafayev and X. Tata, *Monojet plus soft dilepton signal from light higgsino pair production at LHC14*, *Phys. Rev.* **D 90** (2014) 115007 [arXiv:1409.7058] [INSPIRE].

[79] Z. Han, G.D. Kribs, A. Martin and A. Menon, *Hunting quasidegenerate Higgsinos*, *Phys. Rev.* **D 89** (2014) 075007 [arXiv:1401.1235] [INSPIRE].

[80] C. Han et al., *Probing Light Higgsinos in Natural SUSY from Monojet Signals at the LHC*, *JHEP* **02** (2014) 049 [arXiv:1310.4274] [INSPIRE].

[81] A.G. Delannoy et al., *Probing Dark Matter at the LHC using Vector Boson Fusion Processes*, *Phys. Rev. Lett.* **111** (2013) 061801 [arXiv:1304.7779] [INSPIRE].

[82] M.J. Dolan, S. Krippendorf and F. Quevedo, *Towards a Systematic Construction of Realistic D-brane Models on a del Pezzo Singularity*, *JHEP* **10** (2011) 024 [arXiv:1106.6039] [INSPIRE].

[83] S. Krippendorf, M.J. Dolan, A. Maharana and F. Quevedo, *D-branes at Toric Singularities: Model Building, Yukawa Couplings and Flavour Physics*, *JHEP* **06** (2010) 092 [arXiv:1002.1790] [INSPIRE].

[84] A. Maharana and E. Palti, *Models of Particle Physics from Type IIB String Theory and F-theory: A Review*, *Int. J. Mod. Phys.* **A 28** (2013) 1330005 [arXiv:1212.0555] [INSPIRE].

[85] W. Porod, *SPheno, a program for calculating supersymmetric spectra, SUSY particle decays and SUSY particle production at e^+e^- colliders*, *Comput. Phys. Commun.* **153** (2003) 275 [hep-ph/0301101] [INSPIRE].

[86] W. Porod and F. Staub, *SPheno 3.1: Extensions including flavour, CP-phases and models beyond the MSSM*, *Comput. Phys. Commun.* **183** (2012) 2458 [arXiv:1104.1573] [INSPIRE].

[87] G. Bélanger, F. Boudjema, A. Pukhov and A. Semenov, *MicrOMEGAs 3: A program for calculating dark matter observables*, *Comput. Phys. Commun.* **185** (2014) 960 [arXiv:1305.0237] [INSPIRE].